DOI: 10.1002/chem.201100711

Mechanisms and Efficiency of the Simultaneous Removal of Metals and Cyanides by Using Ferrate(VI): Crucial Roles of Nanocrystalline Iron(III) Oxyhydroxides and Metal Carbonates

Jan Filip,[a] Ria A. Yngard,[b] Karolina Siskova,[a] Zdenek Marusak,[a] Vojtech Ettler,[c] Petr Sajdl,[d] Virender K. Sharma,*[b] and Radek Zboril*[a]

Abstract: The reaction of potassium ferrate(VI), K_2FeO_4, with weak-acid dissociable cyanides—namely, $K_2[Zn(CN)_4]$, $K_2[Cd(CN)_4]$, $K_2[Ni(CN)_4]$, and $K_3[Cu(CN)_4]$—results in the formation of iron(III) oxyhydroxide nanoparticles that differ in size, crystal structure, and surface area. During cyanide oxidation and the simultaneous reduction of iron(VI), zinc(II), copper(II), and cadmium(II), metallic ions are almost completely removed from solution due to their coprecipitation with the iron(III) oxyhydroxides including 2-line ferrihydrite, 7-line ferrihydrite, and/or goethite. Based on the results of XRD, Mössbauer and IR spectroscopies, as well as TEM, X-ray photoelectron emission spectroscopy, and Brunauer–Emmett–Teller measurements, we suggest three scavenging mechanisms for the removal of metals including their incorporation into the ferrihydrite crystal structure, the formation of a separate phase, and their adsorption onto the precipitate surface. Zn and Cu are preferentially and almost completely incorporated into the crystal structure of the iron(III) oxyhydroxides; the formation of the Cd-bearing, X-ray amorphous phase, together with Cd carbonate is the principal mechanism of Cd removal.

Interestingly, Ni remains predominantly in solution due to the key role of nickel(II) carbonate, which exhibits a solubility product constant several orders of magnitude higher than the carbonates of the other metals. Traces of Ni, identified in the iron(III) precipitate, are exclusively adsorbed onto the large surface area of nanoparticles. We discuss the relationship between the crystal structure of iron(III) oxyhydroxides and the mechanism of metal removal, as well as the linear relationship observed between the rate constant and the surface area of precipitates.

Keywords: cyanides · iron · nanoparticles · nickel · reaction mechanisms

Introduction

Cyanide is a highly toxic substance; it rapidly binds irreversibly to the binuclear α_3-Cu_B site of cytochrome oxidase, which consequently terminates the enzyme-catalyzed reduction of O_2 to H_2O.[1] The uptake of CN^- increases the concentration of intracellular Ca^{II} that ultimately increases reactive oxygen species and inhibits antioxidant defense systems.[2,3] Cyanide poisoning can be fatal; nevertheless, cyanide is still either used or produced in large quantities in metal plating, mining, and in the production of gas and pharmaceuticals.[4] More than a million tons of cyanide are produced annually worldwide, and a number of accidental leaks and spills of cyanide have had disastrous consequences.[5] The World Health Organization has suggested 1.9 μM to be the maximum acceptable level of cyanide in drinking water.[6] New techniques have therefore been developed to detect low levels of cyanide and to detoxify cyanide in water.[7–9] Cyanide in solution exists in three forms: the free form, for example, HCN, CN^-; as a weak-acid dissociable form (WAD), for example, complexes of Cu, Zn, Cd, and Ni; and as strong-acid dissociable (SAD) cyanides, for example, complexes of Fe, Co, and Ag.

An important environmental and technological consideration is that the treatment of cyanides requires not only the detoxification of cyanide per se, but also the simultaneous removal of toxic metals from the treated water. Consequently, the search for a simple, cost-effective, and environmental-

[a] Dr. J. Filip, Dr. K. Siskova, Z. Marusak, Prof. R. Zboril
Regional Centre of Advanced Technologies and Materials
Palacký University in Olomouc, 17. listopadu 12
771 46 Olomouc (Czech Republic)
Fax: (+420) 585-634-947
E-mail: zboril@prfnw.upol.cz

[b] Dr. R. A. Yngard, Prof. V. K. Sharma
Chemistry Department, Florida Institute of Technology
150 West University Boulevard
Melbourne, Florida 32901 (USA)
Fax: (+1) 321-674-7310
E-mail: vsharma@fit.edu

[c] Dr. V. Ettler
Institute of Geochemistry
Mineralogy and Mineral Resources, Charles University
Albertov 6, 128 43 Prague 2 (Czech Republic)

[d] Dr. P. Sajdl
Department of Power Engineering
Institute of Chemical Technology, Technická 5
166 28 Prague (Czech Republic)

Supporting information for this article is available on the WWW under http://dx.doi.org/10.1002/chem.201100711.

ly friendly technique that allows the simultaneous removal of cyanides and potentially toxic metals is currently one of the most important challenges of water-treatment chemistry.

Various known procedures detoxify cyanides, including physical adsorption, complexation, heterogeneous photocatalysis, and chemical oxidation.[7,10,11] With the exception of oxidation, all these techniques produce highly concentrated waste products that still contain toxic cyanides. Chlorine, hypochlorite, hydrogen peroxide, ozone, sulfur dioxide, and ammonium bisulfite are common chemical oxidants for cyanide destruction, but these oxidants either generate toxic intermediates/products (e.g., cyanogen in chlorination) or are not very efficient.[11,12] Moreover, with these techniques, the simultaneous removal of cyanides and metals is almost impossible.

In recent years, oxidants based on iron in high oxidation states, which have been produced in iron–tetraamido macrocyclic ligand complexes (Fe–TAML)/H_2O_2 or as a salt (e.g., K_2FeO_4), have shown promise as efficient degraders and detoxifiers of various pollutants including estrogens, degradation bisphenols, Orange II dye, and bacterial spores.[13,14] These oxidants have the advantage of being classified as 'green chemistry' and are able to oxidize persistent organic pollutants and kill hardy pathogens.[15,16] Importantly, ferrate ion (FeO_4^{2-}) can induce the coprecipitation of metals, nonmetals, radionuclides, and organics, because the ferric ion, produced by the reduction of ferrate(VI), acts as an efficient coagulant. The most important example of this is the use of iron(VI) for the removal of arsenic, which is otherwise not efficiently removed using common coagulants such as ferric chloride and alum.[17]

Recent studies have used the oxidation of weak-acid dissociable cyanides by using K_2FeO_4 and have demonstrated the possibility of detoxifying cyanide to cyanate and removing metals from the treated water as seen in Equations (1) and (2):

$$5\,HFeO_4^- + [Cu(CN)_4]^{3-} + 8\,H_2O \rightarrow 5\,Fe(OH)_3 + Cu^{II} + 4\,NCO^- + {}^3/_2\,O_2 + 6\,OH^- \quad (1)$$

$$4\,HFeO_4^- + [M(CN)_4]^{2-} + 6\,H_2O \rightarrow 4\,Fe(OH)_3 + M^{II} + 4\,NCO^- + O_2 + 4\,OH^- \quad (2)$$

in which M = Zn, Cd, and Ni.[18,19] However, these studies do not address the efficiency and possible mechanisms of metal removal. Indeed, the chemical composition, crystallinity, size, structure, and surface properties of iron(III) oxide/hydroxide precipitates should control or reflect the mechanisms and kinetics of metal removal. The particle size of precipitates is critically important because some iron oxide polymorphs are generally thermodynamically stable only at the nanoscale.[20] Furthermore, the crystallinity (amorphicity) of solid precipitates also influences the process efficiency of metal removal from solution as the structural incorporation of metals is driven by the degree of development of periodic crystal lattices.[21]

The present work was stimulated by the idea that ferrate(VI) technology seems to be a promising approach for the simultaneous decontamination of toxic cyanides and metals from water; however, there is still a big gap in our understanding of the mechanisms and efficiency of metal removal. Moreover, our preliminary findings clearly showed that iron(VI) was unable to remove Ni^{II} from solution, whereas Cu^{II}, Zn^{II}, and Cd^{II} ions were completely transferred from solution to solid precipitates. This article thus aims: 1) to describe the nature and properties of the iron(III) phase(s) formed in the oxidation of WADs (Cu, Zn, Cd, Ni) by iron(VI) and to relate these properties to the mechanisms and kinetics of metal removal from solution; 2) to determine the role of carbonates in the coprecipitation of metals to learn the causes of the Ni^{II} anomaly; and 3) to evaluate the possibility of leaching metal ions from the precipitates in water as an important environmental aspect related to the location of metal ions on the surface or within the crystal lattice of iron(III) precipitates. Generally, the data presented in this paper are likely to be of great importance in furthering our understanding of the mechanisms of metal coprecipitation with iron(III) oxides, which would occur not only during iron(VI) waste water treatment but also during modern reductive technologies based on the application of zero-valent iron nanoparticles leading to the formation of secondary iron(III) oxides,[22,23] as well as during targeted processes based on the application of iron(III) oxide itself.[24–26]

Results and Discussion

Efficiency of metal removal; surface properties of precipitates versus reaction kinetics: All aqueous solutions that contain weak-acid dissociable cyanides of Zn, Cd, Ni, and Cu were analyzed by atomic absorption spectrometry (AAS) prior to and after treatment with potassium ferrate (Table 1). Whereas comparable concentrations of metal ions (in units of $mg\,L^{-1}$) were detected before the oxidative treatment, all metal ions except Ni decreased by several orders of magnitude after the oxidative treatment with K_2FeO_4. Thus, oxidation of weak-acid dissociable cyanides by ferrate can be considered to be a highly efficient process for the re-

Table 1. Chemical composition of reaction solutions before and after ferrate(VI) treatment, and of solid precipitates (including BET surface area data for solid precipitates).

Cyanide	Composition of reaction solutions before treatment [$mg\,L^{-1}$]	Composition of reaction solutions after treatment [$mg\,L^{-1}$]	Composition of precipitate [wt% of metals]	Surface area [$m^2\,g^{-1}$]
$K_2[Zn(CN)_4]$	1.55 (Zn)	< 0.02 (Zn)	14.72 (Zn)	74
$K_2[Cd(CN)_4]$	2.45 (Cd)	< 0.02 (Cd)	18.14 (Cd)	80
$K_2[Ni(CN)_4]$	1.26 (Ni)	1.22 (Ni)	1.55 (Ni)	88
$K_3[Cu(CN)_4]$	1.59 (Cu)	< 0.04 (Cu)	11.25 (Cu)	183

moval of Zn, Cd, and Cu ions from the solution, but a low-efficiency process for the removal of Ni ions.

The chemical composition of filtered and air-dried precipitates (Table 1) revealed them to contain high concentrations of Cu, Zn, and Cd (11.25, 14.72, and 18.14 wt%, respectively), but only a low content of Ni (<1.55 wt%). This agrees well with the AAS results obtained from the reaction solutions after treatment with K_2FeO_4, for which the removal of Cu, Cd, and Zn from the aqueous solutions during co-precipitation with iron was better than 95%, whereas a decrease of only approximately 3% was observed for Ni. These results thus reflect the anomalous nature of Ni with respect to its removal from the reaction solution. Since the removal of metals on preformed iron(III) oxyhydroxides is generally significantly lower than that precipitated in situ, the process of in situ iron precipitation might represent an effective tool for the sequestration of dissolved metal.[25] The increased level of metal removal by the in situ precipitation process can be explained by an increase of both number of adsorption sites and surface area, when present together with polymerized iron(III) oxyhydroxides.[25]

Concerning the surface properties, all WAD cyanide reaction products had comparable active surface areas (74 to 88 $m^2 g^{-1}$) except for the Cu-bearing precipitate (183 $m^2 g^{-1}$) (Table 1). The variation in surface area was found to be related to the kinetics of the reaction of iron(VI) with cyanide (rate constants were adopted from previously published studies;[19,27,28] Figure 1). Evidently, the slower reaction rate

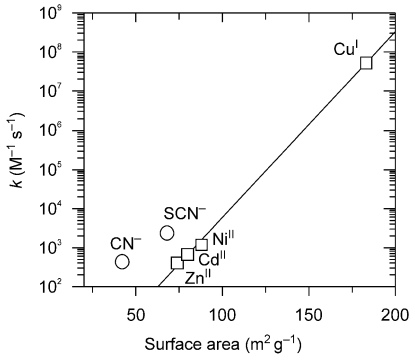

Figure 1. The rate constants of reactions of weak-acid dissociable cyanides with ferrate(VI) (adopted from previously published studies[19,27,28]) versus surface area of individual precipitates.

is reflected in a smaller surface area, whereas the high reaction rate of iron(VI) with $[Cu(CN)_4]^{3-}$ led to the large surface area of the solid reaction product. Interestingly, such variation of active surface area displayed nearly linear behavior with respect to reaction rate constants for WADs (Figure 1). On the other hand, the precipitates obtained in the reaction of free potassium cyanide and thiocyanate (blank samples) gave the lowest surface areas (42 and 67 $m^2 g^{-1}$, respectively), which, however, did not fall on the linear curve of Figure 1. This suggests that metal ions in WADs considerably affect the mechanisms and kinetics of cyanide oxidation and hence the formation of iron(III) precipitates. The reaction kinetics seems to be the key factor in determining the surface area of the precipitates.

Although $[Ni(CN)_4]^{3-}$ also lies on the linear curve (Figure 1), the mechanism of formation of the Ni precipitate should be different. The differences in mechanisms of formation of iron(III) precipitates are, moreover, reflected in the nature of Brunauer–Emmett–Teller (BET) adsorption–desorption isotherms (Figure S1 in the Supporting information). Whereas the precipitates that result from oxidative treatments of $K_2[Ni(CN)_4]$, $K_3[Cu(CN)_4]$, and $K_2[Zn(CN)_4]$ are almost pore-free (no hysteresis), the Cd-bearing precipitate was in fact mesoporous as demonstrated by a large degree of hysteresis in the adsorption–desorption isotherms. To understand differences in the efficiency of metal removal and surface properties of precipitates, we performed a detailed characterization. As a result, the data presented and discussed below provide new insights into the mechanisms of metal removal including an explanation of the anomalous behavior of $[Ni(CN)_4]^{3-}$ during treatment with ferrate(VI).

Differences in composition, structure and morphology of precipitates; mechanisms of metal removal: Due to the fact that all precipitates contained iron as the main component, they were characterized in detail by means of ^{57}Fe Mössbauer spectroscopy, which is sensitive to both the valence and spin state of iron. The measurements were performed at 300 and 25 K (Figure S2 in the Supporting information). The dominant doublet in all room-temperature Mössbauer spectra corresponds to the octahedrally coordinated iron(III) ion in a high-spin state. The results of Mössbauer spectroscopy also illustrate the fact that all the iron atoms are reduced to iron(III) after completion of the reaction of K_2FeO_4 with WADs. Room-temperature and low-temperature spectra as well as corresponding hyperfine parameters are typical for ferrihydrite[29] (average values for room-temperature spectra: isomer shift $\delta = 0.34\ mm\,s^{-1}$ and quadrupole splitting $\Delta E_Q = 0.56\ mm\,s^{-1}$ for doublet 1 and $\delta = 0.33\ mm\,s^{-1}$, $\Delta E_Q = 0.94\ mm\,s^{-1}$ for doublet 2; average values for 25 K spectra: $\delta = 0.44\ mm\,s^{-1}$, quadrupole shift $\varepsilon_Q = -0.04\ mm\,s^{-1}$, hyperfine magnetic field $B_{hf} = 46.9$ T). Moreover, the subspectrum with hyperfine parameters typical for nanocrystalline goethite (RT: $\delta = 0.38\ mm\,s^{-1}$, $\varepsilon_Q = -0.18\ mm\,s^{-1}$, $B_{hf} = 30.5$ T; 25 K: $\delta = 0.45\ mm\,s^{-1}$, $\varepsilon_Q = -0.16\ mm\,s^{-1}$, $B_{hf} = 50.6$ T) is easily recognized in the precipitate of reference samples.[30]

According to the XRD results (Figure 2), all the studied precipitates were mainly composed of nanocrystalline iron(III) oxyhydroxides including goethite (α-FeOOH), 2-line ferrihydrite (2LFh), and 7-line ferrihydrite (7LFh). Nanoparticulate goethite prevailed in the reference samples (Figure S3 in the Supporting information) and was also present as a minor phase in the precipitate that resulted from the reaction between $[Ni(CN)_4]^{2-}$and FeO_4^{2-}. On the other hand, 2LFh dominated in all the metal-bearing precipitates studied, in accordance with Mössbauer data. Two-line ferrihydrite was the only phase after the oxidative treatment of $[Cu(CN)_4]^{3-}$, whereas the oxidation of both $[Zn(CN)_4]^{2-}$and $[Ni(CN)_4]^{2-}$ resulted in a mixture of 2LFh and 7LFh. The

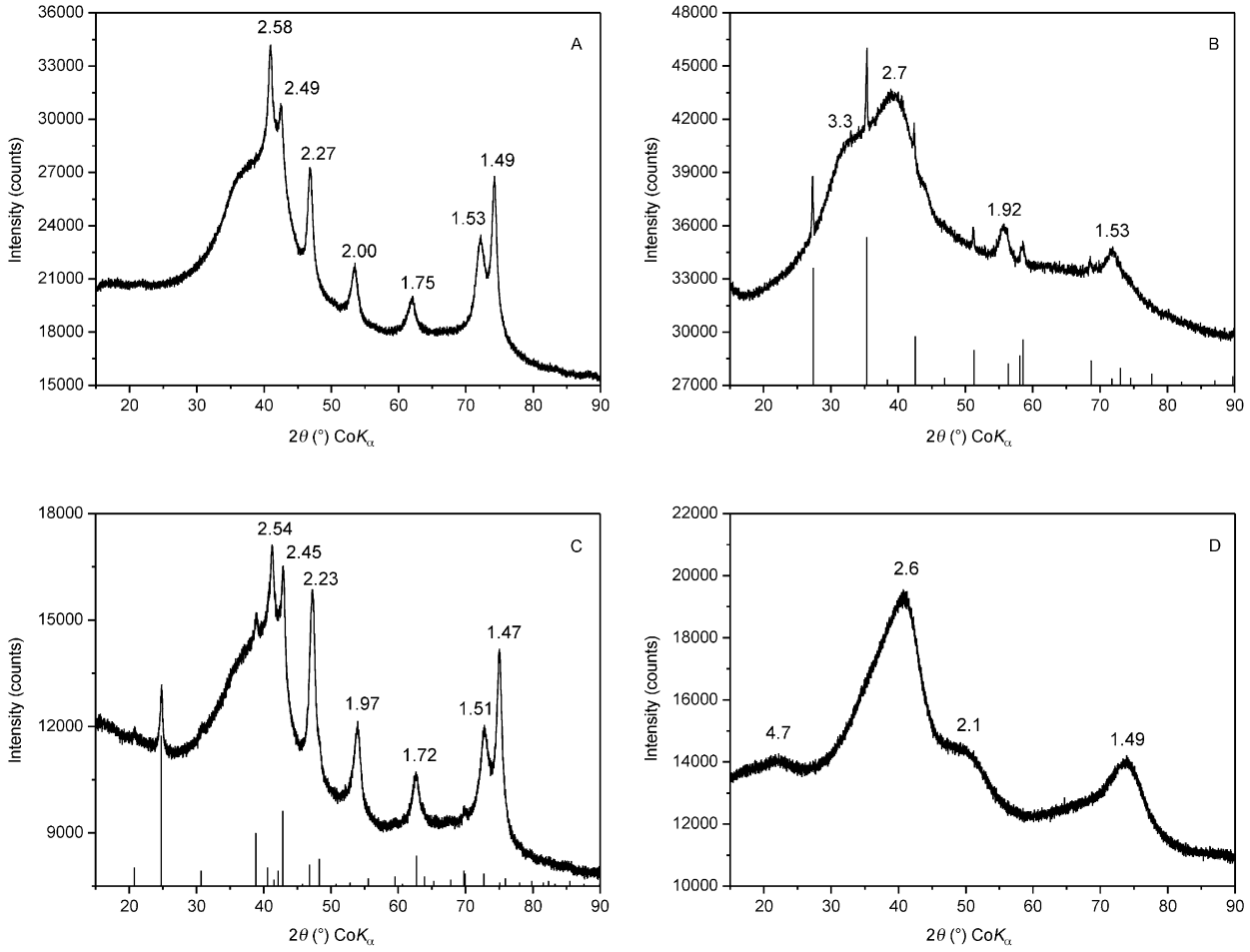

Figure 2. X-ray diffraction patterns of solid precipitates obtained by the reaction of the FeO_4^{2-} ion with cyanides: A) $[Zn(CN)_4]^{2-}$, B) $[Cd(CN)_4]^{2-}$, C) $[Ni(CN)_4]^{2-}$, D) $[Cu(CN)_4]^{3-}$. The lines in pattern B indicate diffractions of $CdCO_3$ (PDF card no. 01-072-1939), whereas the lines in pattern C correspond to the diffractions of goethite (card no. 00-029-0713). Other peaks can be assigned to either 2LFh or 7LFh.

formation of 7LFh, a rarely observed form of ferrihydrite, implies that the ferrihydrite structure is partially stabilized by other elements of ionic radii comparable to iron.[31,32] We can therefore deduce that goethite predominantly crystallizes in systems that contain no metals other than ferric iron under the conditions of the reaction of potassium ferrate(VI) with weak-acid dissociable cyanides. This corresponds well with its presence in reference samples, whereas divalent metals, such as Zn, Cd, and Cu, cause the formation of both 2LFh and 7LFh ferrihydrites.

The Cd-bearing precipitate appears to be anomalous in light of the XRD results (Figure 2). The character of the extremely broad and asymmetric diffraction peaks differs from those typical of 2LFh and implies the presence of highly substituted ferrihydrite and/or the presence of a separate Cd-bearing and X-ray amorphous phase together with 2LFh. In addition to the X-ray amorphous phases, quite sharp diffractions that correspond to $CdCO_3$, known as the mineral otavite, are clearly identified in the Cd-bearing precipitate (Figure 2). Thus, the formation of cadmium carbonate as a single phase evidently represents an important mechanism of cadmium removal. From this viewpoint, it is worth mentioning that metal carbonates were not identified in any of the other precipitates studied. The general role of carbonates in the reaction system is discussed below.

In the TEM images (Figure 3), all studied precipitates except the Cd-bearing precipitate were found to have morphologies typical of ferrihydrites ($\approx$5 nm small particles forming globular aggregates of 20 to 300 nm in diameter) and nanoparticulate goethite (Figure S4 in the Supporting information).

The Cd-bearing sample also appears to be morphologically different. The anomaly in this sample is demonstrated by the presence of sheetlike structures that overgrow shapeless aggregates of ultrafine ferrihydrite nanoparticles (Figure 3B). This observation clearly demonstrates the formation of separate Cd-bearing phase(s), which are assigned to the X-ray amorphous Cd-bearing phase and to the well-crystallized $CdCO_3$ following XRD analysis. This sheetlike morphology is typical of both Cd-bearing phases.[33,34] The presence of these cadmium-bearing sheetlike phase(s) is probably responsible for the mesoporous nature of the precipitate, as observed in adsorption isotherms (see hysteresis in Figure S1 in the Supporting Information).

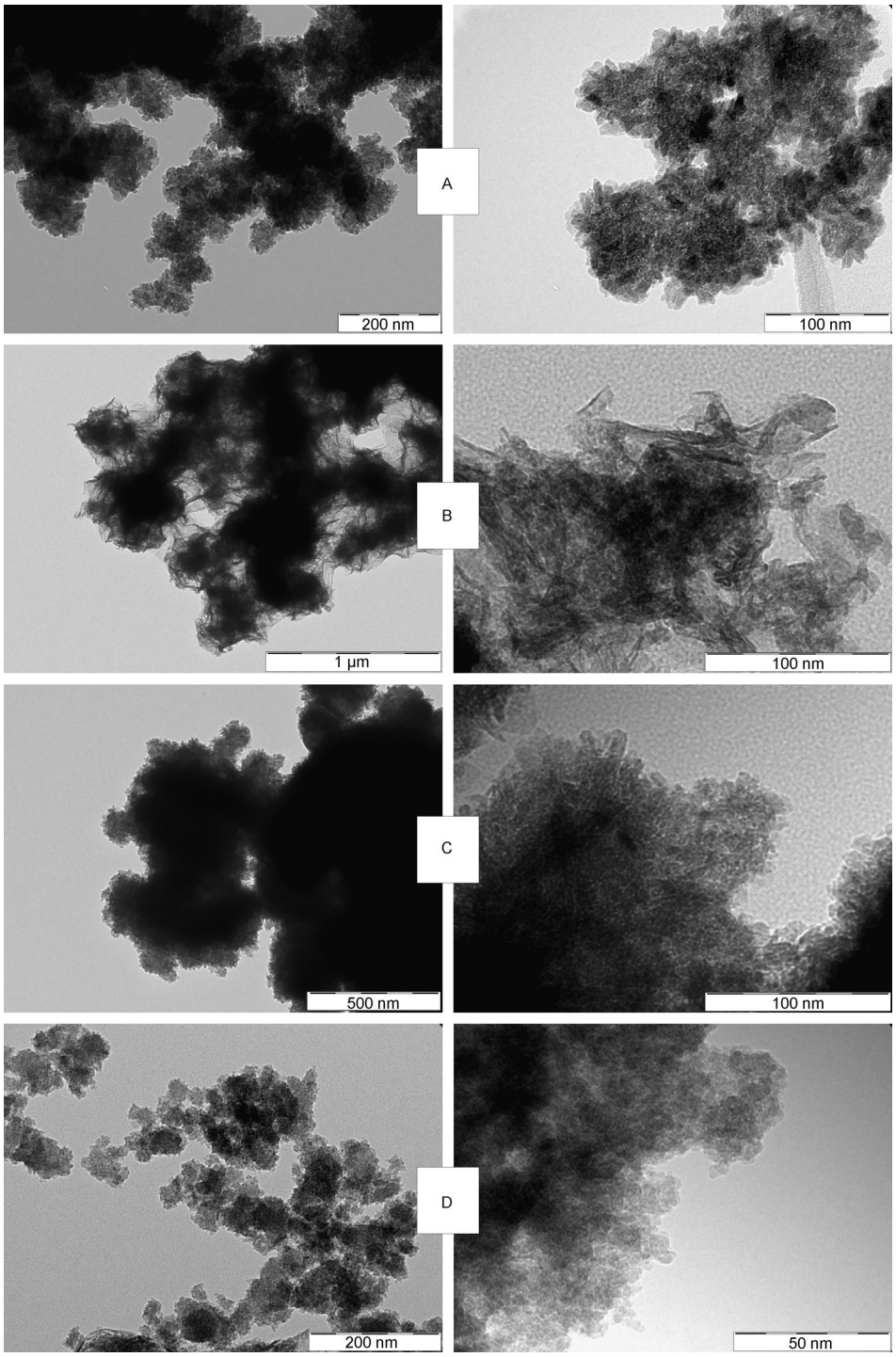

Figure 3. TEM images of solid precipitates obtained by the reaction of the FeO_4^{2-} ion with cyanides: A) $[Zn(CN)_4]^{2-}$, B) $[Cd(CN)_4]^{2-}$, C) $[Ni(CN)_4]^{2-}$, and D) $[Cu(CN)_4]^{3-}$.

Whereas the mechanism of Cd removal during oxidative treatment of $[Cd(CN)_4]^{2-}$ by ferrate(VI) is partly based on the formation of the separate carbonate phase, the mechanisms of Cu and Zn removal seem to be strongly and exclusively related to iron(III) oxyhydroxides. To gain a deeper insight into this relationship, we performed X-ray photoelectron emission spectroscopy (XPS) analysis of precipitates. In the cases of Cu- and Zn-bearing precipitates, XPS analysis of the fresh precipitates revealed rather similar values of metal ion concentrations as in the case of Cd (Table 2). However, a significant increase of Cu and/or Zn concentrations after the sputtering was observed: approximately 38 and 45%, respectively. Thus, a considerably higher content of metals was detected inside the aggregates/particles of precipitates relative to their surfaces. This strongly supports the hypothesis that both Cu and Zn metals are incorporated into the structures of iron(III) oxyhydroxides due to a simultaneous coprecipitation of Fe with Cu or Zn. The lower Fe/metal ratio at the surface of the individual precipitates might be explained by the continued precipitation and partial crystallization of the iron(III) phase, even if Cu(Zn) concentrations in the solution were markedly decreased. This trend was also registered for the Cd-bearing precipitate; however, an increase in Cd concentration after the electron sputtering is less significant (16%). Thus, the structural incorporation is probably the less preferred mechanism of Cd removal along with the above-mentioned mechanism based on the formation of cadmium carbonate.

The low degree of Ni removal from the solution is supported by XPS data measured from the particular precipitate, thus confirming the Ni anomaly as stated earlier. Nickel was predominantly detected in low concentrations at the raw surface of the precipitate, whereas upon sputtering, the Ni concentration dropped to less than half its previous value. We hypothesize that Ni ions are mainly adsorbed on the surface of the iron(III) oxyhydroxide aggregates. Subsequent sputtering induced partial Ni removal from the precipitate surface, hence a significant decrease of Ni content was observed by XPS.

Table 2. Results of XPS analyses for Cu, Zn, Cd, and Ni precipitates.

Sample	Sputtering (t) [min]	Metal concentrations [%] Cu	Zn	Cd	Ni
Cu	0	3.4			
	3	4.7			
Zn	0		2.9		
	3		4.2		
Cd	0			3.1	
	3			3.6	
Ni	0				2.0
	3				0.9

Anomaly of Ni; the crucial role of carbonates in the reaction system: Comparing the reaction rates of $K_2[Ni(CN)_4]$, $K_2[Cd(CN)_4]$, and $K_2[Zn(CN)_4]$,[19,27,28] which are quite similar, the Ni anomaly cannot be explained by slower reaction kinetics. Another possibility is a change in the Ni valence state, which could be important. The valence state of Ni was therefore evaluated by the dimethylglyoxime (dmg)[35] method before and after the treatment with K_2FeO_4. The measurements gave unequivocal evidence for Ni^{2+}, because a yellow precipitate of $[Ni(dmg)_2]$ was formed. Hence, we can exclude the influence of a different valence state of Ni on its preferential presence in the soluble state after the reaction of $K_2[Ni(CN)_4]$ with potassium ferrate(VI). Thus, taking into account the proven role of carbonate in the case of Cd-bearing precipitates (formation of solid $CdCO_3$ phase) and the well-known fact that alkaline solutions spontaneously react with carbon dioxide from the air to form bicarbonates and carbonates, we investigated their possible presence in the reaction solutions by using FTIR absorption spectroscopy, after removal of the solid precipitates (Figure 4). As can be clearly seen in Figure 4, the supernatants of the blank sample (reaction solution from treatment of KCN by K_2FeO_4) and those remaining after the removal of Cu- and Cd-bearing precipitates resulted in spectra that were almost the same as those attributable to bicarbonates.[36] No signal of soluble carbonates was detected in IR spectra of these air-dried supernatants. In fact, in the case of the Ni supernatant, there were at least two bands (positioned at 1415 and 880 cm^{-1}) that matched the characteristic carbonate vibrations, an observation corroborated by direct comparison with the IR absorption spectrum of sodium carbonate (see Figure 4). Thus, we obtained strong experimental proof that highly soluble Ni carbonate alone can serve as a potential factor that induces an Ni anomaly. Indeed, $NiCO_3$ exhibits a solubility product constant several orders of magnitude higher than those of the carbonates of the other metals.[37]

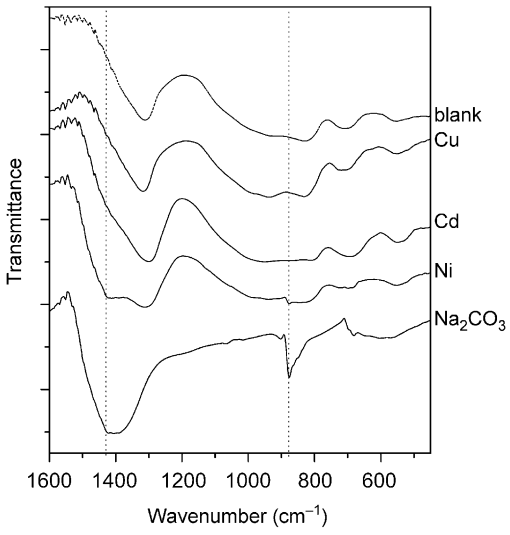

Figure 4. FTIR spectra of solid residues of air-dried supernatants obtained after the microfiltration of particular precipitates. The FTIR spectrum of Na_2CO_3 is given for comparison. Dotted lines are used as visual aids for the sake of clarity.

To quantify the role of carbonates in the reaction systems, we performed theoretical calculations based on the solubility products of particular hydroxides and carbonates (see the Supporting Information). These simplified calculations show that Cu^{II} and Zn^{II} can be removed from the reaction mixture in the form of hydroxides at very low concentrations, which are between three and even six orders of magnitude lower than the concentrations of Cd^{II} and Ni^{II}. This readily explains the coprecipitation of Cu and Zn with iron(III) oxyhydroxides during oxidative treatment of WAD cyanides with ferrate(VI). Furthermore, Cd^{II} and Ni^{II} can remain in solution at relatively high concentrations; consequently, carbonates can compete well with hydroxides as evidenced by the XRD and IR data. However, the calculated concentrations of carbonates required for the precipitation of particular metal carbonates are four orders of magnitude lower in the case of $CdCO_3$ relative to the concentrations required for the precipitation of $NiCO_3$. This corresponds well with the XRD identification of solid $CdCO_3$ in the precipitate, whereas $NiCO_3$ remains predominantly in solution, which would be the principal reason for a low efficiency of Ni removal during treatment of $K_2[Ni(CN)_4]$ by ferrate. With respect to the crucial role of metal carbonates, we should point out that there are at least three sources of carbonates and bicarbonates in the reaction system: 1) the air CO_2, 2) carbonates formed in the aged aqueous solutions of cyanates according to Equation (3):[38]

$$3\,OCN^- + 3\,H_2O \rightarrow H_2NCO_2^- + (NH_2)_2CO + CO_3^{2-} \qquad (3)$$

and 3) carbonates formed by partial hydrolysis of ferrates used for the oxidation of WADs.[39]

It can thus be concluded that Ni remains in the reaction solution in the form of Ni^{II} carbonate, as confirmed by the dimethylglyoxime method and IR absorption spectroscopy. Although this demonstrates that potassium ferrate(VI) effectively decomposes the $K_2[Ni(CN)_4]$, the resulting Ni^{II} ions are almost exclusively preserved in the reaction solution due to the formation of highly soluble carbonate. This interesting reaction mechanism indicates difficult simultaneous removal of cyanides and nickel during treatment with ferrate(VI). However, for the real environmental applica-

tions, the excess amount of carbonates would be added into the reaction solution to induce massive precipitation of nickel carbonates, which would lead to a removal of the majority of Ni from the reaction solution.

Leaching of metals from precipitates; environmental impact: In the previous sections, we have clearly confirmed the efficient removal of Zn, Cd, and Cu ions from solution during the oxidative treatment of weak-acid dissociable cyanides by using ferrate(VI). For real environmental applications of this technique that allows for the simultaneous removal of metals and cyanides, it is necessary to check the possibility of reversible metal release from the precipitates. We therefore performed leaching experiments using deionized water and ethylenediaminetetraacetic acid (EDTA) as a well-known chelating agent. We show that these data are important from the point view of environmental chemistry as well as for a deeper understanding of the mechanisms of metal sequestration by a particular precipitate.

The extractabilities of Zn, Cd, and Cu ions from the particular precipitates are depicted in Figure 5 (for the sake of clarity, the *y* axis is drawn on a logarithmic scale). Cadmium

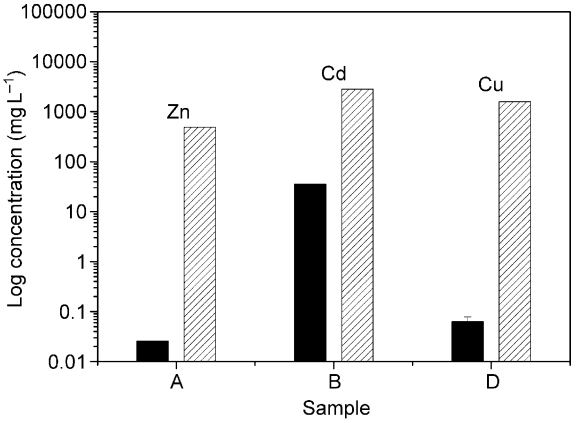

Figure 5. Extractabilities of metals (Zn, Cd, and Cu) from particular iron(III) precipitates as obtained after water (black bars) and 0.05 M EDTA extractions (shaded bars).

was found to be very mobile as evidenced by the presence of 35 mg L^{-1} in the aqueous leachate and nearly 3000 mg L^{-1} in the EDTA leachate. In contrast, Cu and Zn were found to be more tightly bound to the precipitates as evidenced by their low concentrations in water leachates (6.3 and 2.6 μg^{-1}, respectively). The effect of complexation with EDTA on Cu- and Zn-bearing precipitates is indicated by the concentrations of Zn and Cu in EDTA leachates being up to five orders of magnitude higher than their water leachates. Generally, it can be seen that Zn and Cu are thoroughly incorporated into the structures of the iron(III) oxyhydroxides that are formed during the oxidative treatment of particular cyanides with ferrate(VI). As a result, the reversible aqueous induced release of Zn and Cu metals from precipitates is negligible, which demonstrates significant environmental consequences. In comparison, the release of Cd is considerably greater, which is evidently due to the different chemical nature of cadmium and its partial presence in the precipitate as cadmium carbonate. In deionized water (which is known to have a slightly acidic pH) and/or in EDTA (for which an acidic pH is generated by the release of two protons when the complexation of Cd^{II} takes place), the solubility of $CdCO_3$ is relatively higher than it is at alkaline pH. This dependence on pH might be a possible reason for the reversible release of cadmium from the precipitates in leaching experiments.

We should note that the determined concentrations of Ni were nearly the same in both aqueous and EDTA leachates (data not shown). This indicates nearly the same availability of Ni cations for water and EDTA on the precipitate surface. This phenomenon is related to a weak sorption of traces of Ni onto the precipitate surface as expected with respect to the above-mentioned XPS data.

In summary, the results of the leaching experiments not only confirm principal differences in the mechanisms of incorporation of the investigated metal cations, in particular precipitates, they also provide a clear indication of the environmental applicability of ferrate(VI) technology for the simultaneous removal of cyanides and metals. For this application, the most promising data were obtained in the case of the treatment of copper and zinc cyanides.

Conclusion

According to our previous studies,[19,27,28] weak-acid dissociable cyanides are oxidized by ferrates(VI) at alkaline pH, to form iron(III) oxyhydroxides and cyanates. Data summarized in the present study have provided unambiguous proof that ferrate(VI) technology can be used as an environmentally friendly approach for the simultaneous detoxification of cyanides and metals, although the mechanisms and efficiency of metal removal differ considerably.

In the case of $K_2[Zn(CN)_4]$ and $K_3[Cu(CN)_4]$, the metals can be completely removed from solution as they are thoroughly incorporated into the structures of two-line and seven-line ferrihydrites; in this state, it is rather impossible that they can be released from the precipitates into the water.

In the case of $K_2[Cd(CN)_4]$ and $K_2[Ni(CN)_4]$, particular metal carbonates play a key role. X-ray amorphous Cd-bearing phase and $CdCO_3$ were identified as separate phases in the precipitate, which exhibits a mesoporous nature, probably due to the sheetlike morphology of the Cd-bearing phase(s) that surround the ferrihydrite nanoparticles. Most probably, there is also some portion of Cd ions incorporated into the ferrihydrite crystal structure. Despite combined mechanisms, cadmium can also be removed from solution in significant quantities by ferrate(VI) at alkaline pH; however, a significant proportion of cadmium can be reversibly released into water at neutral to acid pH. The negligible removal of Ni^{II} is also related to the formation of carbonate,

which, however, remains in solution in this case, as evidenced by experimental data and theoretical calculations. This Ni anomaly is also reflected in the phase composition of the precipitate in which goethite appears along with ferrihydrite. The traces of Ni identified in the precipitate are probably sorbed onto its surface.

Experimental Section

Materials and reaction mixtures: Potassium zinc(II) tetracyanide ($K_2[Zn(CN)_4]$) and potassium cadmium(II) tetracyanide ($K_2[Cd(CN)_4]$) were purchased from Antec Inc. Potassium nickel(II) tetracyanide ($K_2[Ni(CN)_4]$) was obtained from Sigma–Aldrich Co., and potassium copper(I) tetracyanide ($K_3[Cu(CN)_4]$) was synthesized in the laboratory.[27] All cyanides were used without further purification. Potassium ferrate (K_2FeO_4) was prepared by the wet oxidation method and had a purity of $>98\,\%$.[40] All solutions were prepared with distilled water that had been passed through an $18.2\,M\Omega\,cm^{-1}$ Milli-Q water purification system. In the experiments, a fixed amount of solid K_2FeO_4 was added to solutions (10 mL) of 0.1 M cyanides at pH 9.0. Molar ratios of iron(VI)/cyanide in solution of each M^{II} cyanides were 1:1, except for copper(I) cyanide, in which the ratio was 1:1.25. As blank samples, KCN and KSCN were used and both reacted at 1:1 molar ratio with iron(VI). At these ratios, weak-acid dissociable cyanides were fully oxidized to cyanate, whereas the metals (in the case of WADs cyanides) were released into ionic forms.[19,27,28] After the completion of the reaction, which was determined by the disappearance of the pink-violet color of the FeO_4^{2-} ion, the samples were filtered and air-dried. The precipitates as well as supernatants of filtration were then subjected to detailed multianalytical characterization. The reproducibility of oxidation of cyanides by means of potassium ferrate and the uniformity of the physical properties of the resulting precipitates were tested on two separate experimental runs.

Instrumentation employed for the analysis of liquid samples: Solutions that contained metal cyanides were analyzed using flame atomic absorption spectrometry (Perkin–Elmer Model 4000) both before and after the treatment with potassium ferrate (i.e., after the reaction and filtration). In the case of the Ni ion, its valence state was determined by the standard dimethylglyoxime test under alkaline conditions.

Instrumentation employed for the analysis of precipitates and solid residues of air-dried supernatants: The metals in solid precipitates were determined by flame atomic absorption spectrometry using the Solar M5 (Pye Unicam) spectrometer after dissolving the solid precipitates in mineral acids. Each sample was measured three times, and the calculated relative error was estimated to be below 1%. X-ray diffraction patterns of powder samples were recorded using an X'Pert PRO (PANalytical, The Netherlands) instrument in Bragg–Brentano geometry with iron-filtered CoK_α radiation (40 kV, 30 mA). Samples were placed on a zero-background and rotating single-crystal Si slides, gently pressed to obtain a sample thickness of about 0.5 mm, and scanned in the 2θ range of 15–90° in steps of 0.017°. The acquired patterns were evaluated using X'Pert HighScore Plus software (PANalytical, The Netherlands), PDF-4+, and ICSD databases. Detailed morphological studies of precipitates were performed using a JEOL JEM-2010 transmission electron microscope equipped with an LaB_6 cathode (accelerating voltage of 200 kV; point-to-point resolution of 0.194 nm). A drop of high-purity distilled water that contained the ultrasonically dispersed particles was placed onto a Holey Carbon film supported by a copper-mesh TEM grid and air-dried at room temperature. Selected area electron diffraction (SAED) and energy dispersive X-ray spectrometry measurements were also employed. The specific surface area of the precipitates was determined by a BET3 method (nonlinear, three parameters, full equation) in the p/p_0 range between 0 and 0.5 using a Coulter SA 3100 BET surface area analyzer with N_2 as the adsorption gas. Samples were degassed at room temperature with a pressure of 10^{-6} Pa for 12 h. The accuracy of the determined specific surface area is ±3%. An Omicron Nanotechnology ESCAProbeP X-ray photoelectron emission spectroscopy system working under ultra-high vacuum conditions ($<10^{-8}$ Torr) and with a monochromated AlK_α X-ray source (1486.7 eV) was used for the qualitative and quantitative chemical analysis of the surface of precipitates (analyzed surface layer of <1 nm, i.e., five atomic layers), as well as depth profiling using sputtering. The spectra of particular metals were measured stepwise with a binding energy step of 0.05 eV. The data were processed using the CasaXPS program. Transmission ^{57}Fe Mössbauer spectra were collected at a constant acceleration mode with a ^{57}Co(Rh) source. Measurements were carried out at 300 and 25 K. A pure α-Fe foil was used as a calibration standard. Fourier transform infrared spectra of solid precipitates and solid residues of air-dried supernatants were recorded using a Nexus 670 FTIR spectrometer (ThermoNicolet) with either KBr pellets (400 to 4000 cm^{-1}), or a Smart Orbit diamond ATR technique (200 to 4000 cm^{-1}).

Leaching of metals from precipitates: Two short-term extraction batch tests were used to determine the possible environmental release of metallic contaminants from solid precipitates: 1) a deionized H_2O purifying system (Millipore Academic, USA), liquid-to-solid (L/S) ratio of 50 representing the most simple extraction medium;[41] and 2) 0.05 M EDTA adjusted to pH 7, L/S ratio of 50, representing a chelating extraction agent commonly used to assess the '(bio)available' content of metals in soils and sediments.[42] Each batch reactor was shaken on an end-over-end shaker (60 rpm) at 22 °C ±3 °C for 2 h. The suspensions were centrifuged for 5 min at 3000 rpm using a 320R centrifuge (Hettich Universal, Germany). Solutions were subsequently filtered through 0.1 μm membrane filters (Millipore, USA) using Sartorius polycarbonate filtration holders to eliminate colloidal particles. The values of pH and Eh were recorded in each extract using Schott Handylab 1 multimeters. The extracts were diluted and analyzed for the concentrations of Fe, Cd, Cu, Ni, and Zn by using inductively coupled plasma mass spectrometry (ICPMS, Thermo XSERIES). Indium was used as an internal standard for ICPMS determinations. The experiment was run in duplicate (two independent reactors for each sample) with procedural blanks. The quality of the ICPMS measurements was controlled using a standard reference material NIST 1460 (trace elements in water). The percentage error of the measurement was <7% relative standard deviation for Fe, <10% for Zn, and <4% for other elements.

Acknowledgements

The authors thank J. Pechousek, P. Kadlec, M. Matikova-Malarova, L. Strnad, and D. Jancik for BET, AAS, FTIR, ICPMS, and TEM measurements, respectively, and Professor Mary Sohn for her useful comments. This work has been supported by the Academy of Sciences of the Czech Republic (KAN115600801); by the Ministry of Education, Youth and Sports of the Czech Republic (MSM 0021620855 and 1M6198959201), and by the Operational Program Research and Development for Innovations: European Social Fund (CZ.1.05/2.1.00/03.0058).

[1] S. C. Lee, M. J. Scott, K. Kauffmann, E. Munck, R. H. Holm, *J. Am. Chem. Soc.* **1994**, *116*, 401–402.
[2] J. D. Johnson, T. L. Meisenheimer, G. E. Isom, *Toxicol. Appl. Pharmacol.* **1986**, *84*, 464–469.
[3] B. K. Ardelt, J. L. Borowitz, G. E. Isom, *Toxicology* **1989**, *56*, 147–154.
[4] M. A. Acheampong, R. J. W. Meulepas, P. N. L. Lens, *J. Chem. Technol. Biotechnol.* **2010**, *85*, 590–613.
[5] R. Koenig, *Science* **2000**, *287*, 1737–1738.
[6] World Health Organization, **1996**.
[7] R. Bhattacharya, S. J. S. Flora in *Handbook of Toxicology of Chemical Warfare Agents* (Ed.: R. C. Gupta), Academic Press, Boston, **2009**, pp. 255–290.
[8] Z. Dai, E. M. Boon, *J. Am. Chem. Soc.* **2010**, *132*, 11496–11503.
[9] J. Jo, D. Lee, *J. Am. Chem. Soc.* **2009**, *131*, 16283–16291.

[10] S. N. Frank, A. J. Bard, *J. Am. Chem. Soc.* **1977**, *99*, 303–304.
[11] C. A. Young in *Cyanide: Social, Industrial and Economic Aspects* (Eds.: C. A. Young, L. G. Twidwell, C. G. Anderson), TMS, Warrendale, **2001**, pp. 175–194.
[12] V. K. Sharma, R. A. Yngard, D. E. Cabelli, J. Clayton Baum, *Radiat. Phys. Chem.* **2008**, *77*, 761–767.
[13] A. Chanda, S. K. Khetan, D. Banerjee, A. Ghosh, T. J. Collins, *J. Am. Chem. Soc.* **2006**, *128*, 12058–12059.
[14] V. K. Sharma, D. E. Cabelli, *J. Phys. Chem. A* **2009**, *113*, 8901–8906.
[15] W. C. Ellis, C. T. Tran, R. Roy, M. Rusten, A. Fischer, A. D. Ryabov, B. Blumberg, T. J. Collins, *J. Am. Chem. Soc.* **2010**, *132*, 9774–9781.
[16] a) V. K. Sharma, *Chemosphere* **2008**, *73*, 1379–1386; b) V. K. Sharma, X. Z. Li, N. Graham, R. A. Doong, *J. Water Supply: Res. Technol.-Aqua* **2008**, *57*, 419–426.
[17] a) Y. Lee, I. Um, J. Yoon, *Environ. Sci. Technol.* **2003**, *37*, 5750–5756; b) A. Jain, V. K. Sharma, M. S. Mbuya, *J. Hazard. Mater.* **2009**, *169*, 339–344.
[18] N. Costarramone, A. Kneip, A. Castetbon, *Environ. Technol.* **2004**, *25*, 945–955.
[19] R. A. Yngard, V. K. Sharma, J. Filip, R. Zboril, *Environ. Sci. Technol.* **2008**, *42*, 3005–3010.
[20] A. Navrotsky, L. Mazeina, J. Majzlan, *Science* **2008**, *319*, 1635–1638.
[21] m. Loan, O. G. M. Newman, J. B. Farrow, G. M. Parkinson, *Cryst. Growth Des.* **2008**, *8*, 1384–1389.
[22] X. G. Li, W. X. Zhang, *J. Phys. Chem. C* **2007**, *111*, 6939–6946.
[23] S. R. Kanel, D. Nepal, B. Manning, H. Choi, *J. Nanopart. Res.* **2007**, *9*, 725–735.
[24] D. A. Dzombak, F. M. M. Morel, *Surface Complexation Modeling: Hydrous Ferric Oxide*, Wiley, New York, **1990**.
[25] K. L. Mercer, J. E. Tobiason, *Environ. Sci. Technol.* **2008**, *42*, 3797–3802.
[26] B. Pan, H. Qiu, B. Pan, G. Nie, L. Xiao, L. Lv, W. Zhang, Q. Zhang, S. Zheng, *Water Res.* **2010**, *44*, 815–824.
[27] V. K. Sharma, C. R. Burnett, R. Yngard, D. Cabelli, *Environ. Sci. Technol.* **2005**, *39*, 3849–3854.
[28] R. Yngard, S. Damrongsiri, K. Osathaphan, V. K. Sharma, *Chemosphere* **2007**, *69*, 729–735.
[29] J. Filip, R. Zboril, O. Schneeweiss, J. Zeman, M. Cernik, P. Kvapil, M. Otyepka, *Environ. Sci. Technol.* **2007**, *41*, 4367–4374.
[30] R. M. Cornell, U. Schwertmann, *The Iron Oxides: Structure, Properties, Reactions, Occurances and Uses*, Willey-VCH, Weinheim, **2003**.
[31] J. L. Jambor, J. E. Dutrizac, *Chem. Rev.* **1998**, *98*, 2549–2585.
[32] M. Soma, H. Seyama, N. Yoshinaga, B. K. G. Theng, C. W. Childs, *Clay Sci.* **1996**, *9*, 385–391.
[33] Z. Jia, Y. Tang, L. Luo, B. Li, *Cryst. Growth Des.* **2008**, *8*, 2116–2120.
[34] M. Chen, L. Gao, *J. Cryst. Growth* **2006**, *286*, 228–234.
[35] C. S. de Sousa, M. Korn, *Anal. Chim. Acta* **2001**, *444*, 309–315.
[36] K. Nakamoto, *Infrared and Raman Spectra of Inorganic and Coordination Compounds, Part A: Theory and Applications in Inorganic Chemistry*, Wiley, New York, **2009**, pp. 185 and 391.
[37] http://www.csudh.edu/oliver/chemdata/data-ksp.htm, 16th February **2011**.
[38] M. H. Brooker, N. Wen, *Can. J. Chem.* **1993**, *71*, 1764–1773.
[39] L. Machala, R. Zboril, V. K. Sharma, J. Filip, D. Jancik, Z. Homonnay, *Eur. J. Inorg. Chem.* **2009**, 1060–1067.
[40] B. H. J. Bielski, M. J. Thomas, *J. Am. Chem. Soc.* **1987**, *109*, 7761–7764.
[41] V. Ettler, M. Mihaljevič, O. Šebek, T. Grygar, *Anal. Chim. Acta* **2007**, *602*, 131–140.
[42] P. Quevauviller, *Trac-Trends Anal. Chem.* **1998**, *17*, 289–297.

Received: March 8, 2011
Published online: July 26, 2011

